International Journal of Pharmaceutics 474 (2014) 95–102

Contents lists available at ScienceDirect

International Journal of Pharmaceutics

journal homepage: www.elsevier.com/locate/ijpharm

Pharmaceutical nanotechnology

Angiopep-2 and activatable cell penetrating peptide dual modified nanoparticles for enhanced tumor targeting and penetrating

Ling Mei, Qianyu Zhang, Yuting Yang, Qin He, Huile Gao *

Key Laboratory of Drug Targeting and Drug Delivery Systems, West China School of Pharmacy, Sichuan University, No. 17, Block 3, Southern Renmin Road, Chengdu 610041, China

ARTICLE INFO

Article history:
Received 14 June 2014
Received in revised form 25 July 2014
Accepted 14 August 2014
Available online 17 August 2014

Keywords:
Glioma
Systemic targeting delivery
Activatable cell penetrating peptide
Angiopep-2

ABSTRACT

Delivering chemotherapeutics by nanoparticles into tumor was influenced by at least two factors: specific targeting and highly efficient penetrating of the nanoparticles. In this study, two targeting ligands, angiopep-2 and activatable cell penetrating peptide (ACP), were functionalized onto nanoparticles for tumor targeting delivery. In this system, angiopep-2 is a ligand of low-density lipoprotein receptor-related protein-1 (LRP1) which was highly expressed on tumor cells, and the ACP was constructed by the conjugation of RRRRRRRR (R8) with EEEEEEEE through a matrix metalloproteinase-2 (MMP-2) sensitive linker, enabling the ACP with tumor microenvironment-responsive cell penetrating property. 4 h incubation of ACP with MMP-2 leads to over 80% cleavage of ACP, demonstrating ACP indeed possessed MMP-2 responsive property. The constructed dual targeting nanoparticles (AnACNPs) were approximately 110 nm with a polydispersity index of 0.231. In vitro, ACP modification and angiopep-2 modification could both enhance the U-87 MG cell uptake because of the high expression of MMP-2 and LRP-1 on C6 cells. AnACNPs showed higher uptake level than the single ligand modified nanoparticles. The uptake of all particles was time- and concentration-dependent and endosomes were involved. In vivo, AnACNPs showed best tumor targeting efficiency. The distribution of AnACNPs in tumor was higher than all the other particles. After microvessel staining with anti-CD31 antibody, the fluorescent distribution demonstrated AnACNPs could distribute in the whole tumor with the highest intensity. In conclusion, a novel drug delivery system was developed for enhanced tumor dual targeting and elevated cell internalization.

1. Introduction

Chemotherapy is one of the most common strategies for managing cancers. However, most chemotherapeutics suffered from poor tumor targeting ability and high drug-originated side effects. Nanoparticulated systems, such as nanoparticles (NPs), could envelope these chemotherapeutics and deliver them to tumor owing to the enhanced permeability and retention (EPR) effect (Fang et al., 2011; Matsumura and Maeda, 1986). The EPR effect emerges because of the incomplete tumor blood vessels caused by the quick growth. To take advantage of the EPR effect, the nanoparticulated systems were fabricated with PEG to improve their blood circulation time, thus the systems could distribute into tumor as much as possible. Nowadays, there are several nanoparticulated drugs available on the market (Barenholz, 2012; Debbage, 2009). Most of them benefit from the EPR effect. However, due to the poor interaction efficiency between these PEGylated nanoparticulated drugs and cells, the distribution in tumor is still modest, thus, the treatment outcome is far from satisfactory.

To improve the targeting efficiency and cell internalization, ligands were often anchored onto the nanoparticulated systems (Florence, 2012; Gao et al., 2013a; van der Meel et al., 2013). Basically, the ligands could be divided into two categories: cell penetrating peptides (CPPs) and active targeting ligands. CPPs are named because of their function to elevate membrane penetration and cell internalization (Foged and Nielsen, 2008; Liu et al., 2013). Although CPPs were widely used to enhance the intracellular delivery of various cargoes and nanoparticles (Foged and Nielsen, 2008; Liu et al., 2014a; Marcucci and Lefoulon, 2004), the poor selection between neoplastic and non-neoplastic cells restricted the in vivo application of them (Alberici et al., 2013; Kondo et al., 2012). To overcome this hurdle, activatable CPPs were constructed. The CPPs were shielded in the blood circulation using peptides or PEG. When they reached the target site, the cover could be detached under certain triggers, such as pH, proteinase, UV light,

* Corresponding author. Tel.: +86 28 85502575; fax: +86 28 85502532.
E-mail address: gaohuile@scu.edu.cn (H. Gao).

http://dx.doi.org/10.1016/j.ijpharm.2014.08.020
0378-5173/

and then the CPPs were exposed (Jiang et al., 2004; Kuai et al., 2011; Olson et al., 2010). Another kind of ligands could be named as active targeting ligands because they could be recognized by specific receptors and carriers which were highly expressed on certain cells such as tumor cells (Bae and Park, 2011; Lammers et al., 2012). These receptors and carriers could interact with the ligands and then trigger the internalization procedure, thus, transporting the nanoparticles into cells. However, the active targeting ligands were characterized with poor internalization efficiency, which restricted the intracellular delivery (Liu et al., 2014b; Svensen et al., 2012). Therefore, new targeting delivery strategy should be developed to improve both the targeting efficiency and internalization capacity.

Dual targeting delivery systems were nanoparticles that were functionalized with two kinds of ligands to fully address the requirement. Thus in this study, we combined the advantages of activatable CPPs and active targeting ligands to construct a more efficient tumor targeting drug delivery systems. Firstly, nanoparticles were functionalized with a kind of activatable CPPs: EEEEEEEE(E8)-6-aminohexanoyl-PLGLAG-RRRRRRRR(R8) (ACP). The cationic R8 were covered by anionic E8 through electrostatic force and a linker (Jiang et al., 2004). The linker, PLGLAG is the substrate of metalloproteinase-2 (MMP-2) (Forsyth et al., 1999; Olson et al., 2010). Therefore, the E8 could be detached and R8 could be exposed in tumor because of the highly expressed MMP-2 in tumor. Then the nanoparticles were further functionalized with angiopep-2. Angiopep-2 is a ligand of low-density lipoprotein receptor-related protein-1 (LRP1) which have been identified to be expressed on cancer cells (Demeule et al., 2008; Ito et al., 2006; Maletinska et al., 2000). Thus angiopep-2 could be used as an active tumor targeting ligand.

In this study, several experiments were performed to explore the targeting delivery effect of angiopep-2 and ACP dual modified nanoparticles (AnACNPs). To track the in vitro and in vivo behaviors, coumarin-6 and DiR, two most commonly used dyes, were loaded into the NPs. The excitation/emission wavelengths of coumarin-6 were 465/502 nm, which was widely used in particle tracking and cell imaging because of its high fluorescent efficiency (Lu et al., 2005). The excitation/emission wavelengths of DiR were 748/780 nm, which was often used for in vivo imaging because of the low fluorescent background of tissues at such high wavelength.

2. Materials and methods

2.1. Materials

Angiopep-2, ACP and R8 were custom synthesized by Sangon Biotech (Shanghai, China). Methoxy poly(ethyleneglycol)-poly (ε-caprolactone) (MPEG-PCL) (Mw: 3k–15k), maleimide poly (ethylene glycol)-poly(ε-caprolactone) (MAL-PEG-PCL) (Mw: 3.4k–15k) and carboxyl poly(ethylene glycol)-poly (ε-caprolactone) (HOOC-PEG-PCL) (Mw: 3.4k–15k) were synthesized as previously described (Pang et al., 2008). Coumarin-6, *N*-(3-dimethylaminopropyl)-*N*′-ethylcarbodiimide hydrochloride (EDC) and *N*-hydroxy-succinimide (NHS) were purchased from Sigma (Saint Louis, MO, USA). DiR was purchased from Biotium (Hayward, CA, USA). Western blot related reagents were purchased from Beyotime (Haimen, China). The U-87 MG cell line was purchased from the Institute of Biochemistry and Cell Biology, Shanghai Institutes for Biological Sciences, Chinese Academy of Sciences (Shanghai, China). bEnd. 3 cell line (from mouse) was obtained from American type culture collection (ATCC) (Manassas, VA, USA). Plastic cell culture dishes and plates were purchased from Cyagen Biosciences Inc. (Guangzhou, China). Dulbecco's modified Eagle's (high glucose) cell culture medium (DMEM) and fetal bovine serum (FBS) were obtained from Life technologies (Grand Island, NY, USA). 4,6-diamidino-2-phenylindole (DAPI) was purchased from Beyotime (Haimen, China). Rabbit anti-CD31 antibody and MMP-2 protein (rat) were obtained from Abcam Ltd. (Hong Kong, China). Alxafluor 488-conjugated goat anti-rabbit secondary antibody was obtained from Jackson Immunoresearch Laboratories, Inc. (West Grove, PA, USA). All other chemicals were purchased from Sinopharm Chemical Reagent (Shanghai, China).

BALB/c nude mice (male, 4–5 weeks, 18–22 g) were obtained from the Animal Research Center of Sichuan University (Chengdu, China) and maintained under standard housing conditions. All animal experiments were carried out in accordance with protocols evaluated and approved by the ethics committee of Sichuan University.

2.2. Preparation and characterization of NPs

The PEG-PCL nanoparticles (NPs) were prepared by an emulsion/solvent evaporation method described previously (Gao et al., 2011). 1 mL of dichloromethane, containing 28 mg of MPEG-PCL, 1 mg of HOOC-PEG-PCL and 1 mg of MAL-PEG-PCL, was added into a tube containing 5 mL of 0.6% sodium cholate hydrate solution. Then the mixture was pulse sonicated for 75 s at 200 W on ice using a probe sonicator (Scientz Biotechnology Co. Ltd. China). Then, the emulsion was applied to a rotary evaporator to remove the dichloromethane and the NPs were condensed to a fixed concentration by ultrafiltration at 4000 × *g*.

For the angiopep-2 conjugation (AnNPs), the carboxyl unit of NP was activated by EDC and NHS for 0.5 h and then reacted with 50 μg of angiopep-2 in 1 mL of PBS (pH 7.4) for 4 h in the dark. For the R8 or ACP conjugation (CNPs, ACNPs and AnACNPs), 50 μg of R8 or ACP was added to the NPs or AnNPs suspension and reacted for 6 h in the dark. The product was then applied to a sepharose CL-4B column to remove the unconjugated peptides and the nanoparticles were collected. Coumarin-6- and DiR-loaded AnACNPs were prepared with the same procedure except that the materials contained 30 μg of coumarin-6 or 300 μg of DiR.

Particle size and zeta potential were determined by dynamic light scattering (DLS) using a Malvern Zeta Sizer (Malvern, NanoZS, UK). After negative staining with 2% sodium phosphotungstate solution, the morphology of AnACNPs was captured by transmission electron microscope (TEM) (H-600, Hitachi, Japan).

2.3. Cleavage studies of ACP

To study the sensitivity of the ACP cleavage by MMP-2, ACP was mixed with MMP-2 at the final concentrations of 180 μg peptide/mL and 18 μg MMP-2/mL and incubated at 37 °C. At different time intervals, the reaction mixture or ACP solution were measured by high-performance liquid chromatography (HPLC). The mobile phase composed of solvent A (water with 0.1% trifluoroaceticacid (TFA)) and solvent B (acetonitrile with 0.1% TFA). The gradient elution was performed as follows: 90% solvent A to 50% solvent A in 18 min, 50% solvent A to 10% solvent A in 2 min. The flow rate was 1 mL/min, and the measurement wavelength was 220 nm.

2.4. Cellular uptake

U-87MG cells in the logarithmic growth phase were seeded in 12-well plates at a density of 1×10^4 cells/mL. 24 h later, 100 μg/mL of coumarin-6-loaded NPs, CNPs, ACNPs, AnNPs or AnACNPs were added into the wells and incubated for 0.25, 1 or 4 h. After washing with ice-cold PBS for 3 times, the fluorescent distribution was directly determined by a fluorescent microscope (Leica, Germany). To determine the effect of concentration on cellular uptake, cells were incubated with 25, 100 or 400 μg/mL of coumarin-6-loaded

NPs, CNPs, ACNPs, AnNPs or AnACNPs for 1 h. And then the fluorescent intensity was determined as described above.

2.5. Subcellular colocalization

U87 cells were seeded in 6 cm glass-bottom dishes at a density of 1×10^4 cells/mL. After 24 h incubation, cells were treated with 100 μg/mL of coumarin-6-loaded NPs, CNPs, ACNPs, AnNPs or AnACNPs for 1 h. 30 min before the incubation ended, cells were added with LysoTracker Red DND-99 (50 nmol/L). After nuclei staining with DAPI (1 μg/mL) for 5 min, the cells were washed, fixed and mounted in fluorescent mounting medium. The fluorescent distribution was captured with a confocal microscope (TCS SP5, Leica, Germany).

2.6. In vivo imaging

100 μL of U87 cells (3×10^7 cells/mL) was injected into the right flank of the nude mice. The tumor volume was determined using the following equation: tumor volume = (length × width^2)/2 (Gao et al., 2013b). When the tumor volume was over 100 mm^3, mice were intravenously administered with 2 mg/kg of DiR-loaded NPs, CNPs, ACNPs, AnNPs or AnACNPs. The distribution of fluorescence was observed by an IVIS spectrum in vivo imaging system (Caliper, MA, USA) 2 h and 24 h post injection. Then the mice were sacrificed at 24 h and the ex vivo image of all the tissues was also captured at that time. The tissues were then applied to slice preparation and nuclei were stained with 1 μg/mL of DAPI for 5 min. The fluorescent distribution was determined using a fluorescent microscope (Leica, Germany).

2.7. Tumor distribution

When the tumor volume was over 100 mm^3, U-87MG xenografts bearing mice were intravenously administered with 2 mg/kg of DiR-loaded NPs, CNPs, ACNPs, AnNPs or AnACNPs. 2 h later, the mice were anesthetized and the hearts were perfused with saline with 4% paraformaldehyde followed. The tumors were removed for 5 μm frozen sections preparation. Microvessel of tumor was stained with rabbit anti-CD31 antibody (1:200) followed with Alexafluor 594 conjugated donkey anti rabbit antibody according to previous established procedure (Gao et al., 2011). After nuclei were stained by 1 μg/mL of DAPI for 5 min, the distribution of fluorescence was observed by a confocal microscope (LSM710, Carl Zeiss, Germany).

3. Results and discussion

3.1. Characterization of AnACNPs

The particle sizes of the particles were all around 110 nm with a narrow distribution (PDI < 0.3, Table 1). The particles of AnACNPs were mostly spherical according to TEM (Fig. 1). The size viewed by TEM was much smaller than that determined by DLS because the DLS size was hydrated particle size while the TEM size was dehydrated size. The nanoparticles with sizes lower than 200 nm may get benefit from the EPR effect of tumors because the cutoff size of most tumors was about 200 nm–1.2 μm (Hobbs et al., 1998). The zeta potentials of all kinds of particles, except CNPs, were around −10 mV. The negative charge of the particles could decrease the serum protein adsorption, resulting in relatively long blood circulation time.

Table 1
Particle size and zeta potential of different nanoparticles.

Formulations	Particle size (nm)	PDI	Zeta potential (mV)
NPs	106.7	0.168	−10.7
CNPs	110.9	0.206	−0.32
ACNPs	113.4	0.211	−9.48
AnNPs	110.2	0.187	−11.2
AnACNPs	114.5	0.231	−10.4

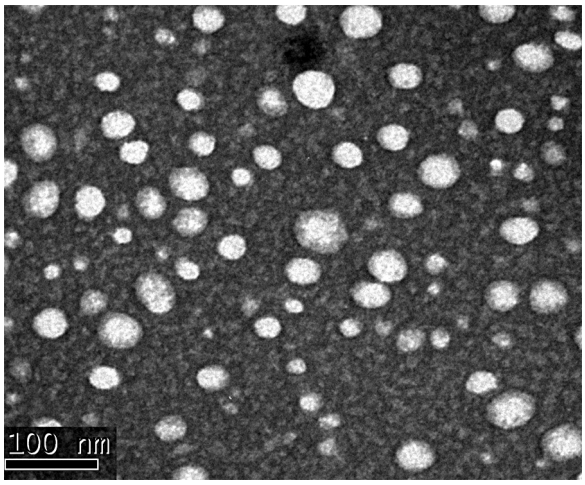

Fig. 1. TEM image of AnACNPs.

3.2. Cleavage of ACP by MMP-2 in vitro

The MMP-2-specific cleavage of ACP was confirmed by MMP-2 hydrolysis experiments in vitro. The cleavage of ACP was observed to be in a time-dependent manner (Fig. 2). With the extension of hydrolysis time, the degree of cleavage improved, and nearly 80% ACP was cleaved after 4 h exposure while the ACP solution without MMP-2 showed little cleavage, which was consistent with previous study (Gao et al., 2013c). Furthermore, the initial cleavage rate reached 60% at 2 h, which demonstrated that the cleavable construct was highly susceptible to MMP-2 and the proteolysis velocity was fast at the beginning. Therefore, the cleavable function of AnACNPs could be realized in cancer cells with MMP-2 expression.

3.3. Cellular uptake

The uptake of various nanoparticles by U-87MG cells showed obviously time- and concentration-dependent manner (Fig. 3), which was consistent with other kinds of nanoparticles (Gao et al., 2013a). The uptake of CNPs was significantly higher than that of

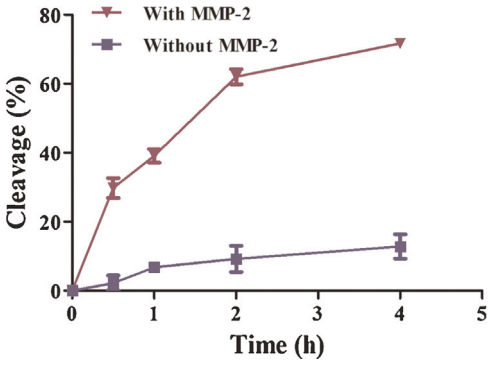

Fig. 2. Cleavage of ACP by MMP-2.

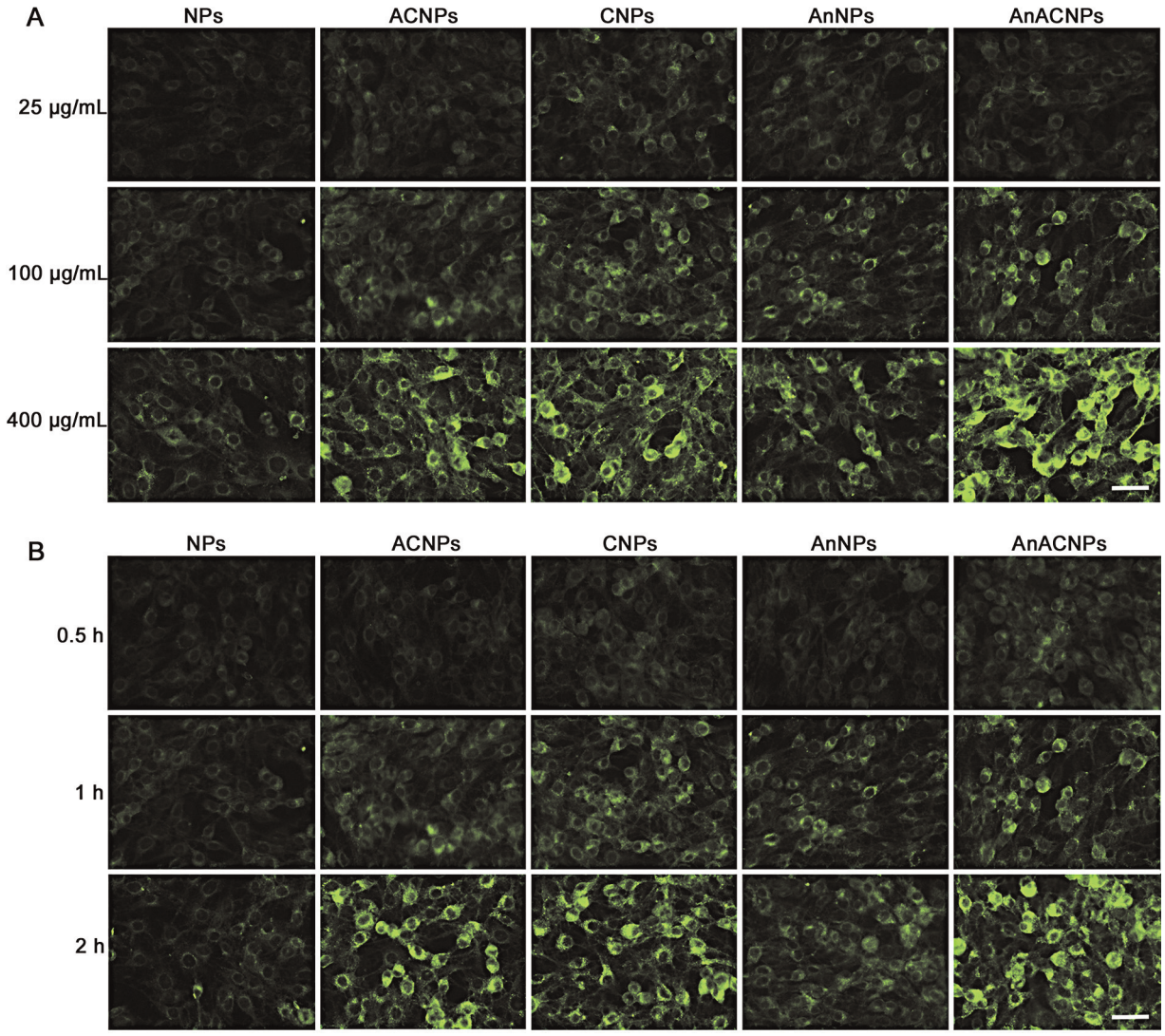

Fig. 3. Cellular uptake of AnACNPs. A: Cellular uptake of different concentrations of coumarin-6-loaded NPs, ACNPs, CNPs, AnNPs and AnACNPs for 1 h. Bar represents 50 μm. B: Cellular uptake of 100 μg/mL of coumarin-6-loaded NPs, ACNPs, CNPs, AnNPs and AnACNPs for different periods of time. Bar represents 50 μm.

NPs, owing to the cell penetrating property of R8 (Gao et al., 2013c). Comparatively, the uptake of ACNP was similar to that of CNPs, suggesting the cell penetrating property could be recovered during the incubation, which was consistent with the high expression of MMP-2 on U-87MG cells. The uptake of AnNPs was also higher than that of NPs, owing to the highly expressed LRP1 on U-87MG cells (Maletinska et al., 2000). LRP1 could specifically recognize angiopep-2 and mediate the internalization of angiopep-2 decorated nanoparticles, which was consistent with previous study (Xin et al., 2011). Combining the specific targeting ability of angiopep-2 and activatable cell penetrating property of ACP, the uptake of AnACNPs was higher than that of ACNPs and AnNPs, suggesting the dual-modification could further improve the tumor targeting efficiency (Gao et al., 2013c; Tang et al., 2013). These results primarily demonstrated AnACNPs was superior to single peptide modified nanoparticles in tumor targeting.

3.4. Subcellular colocalization

The endosomes were labeled by LysoTracker Red to evaluate the colocalization with various nanoparticles (Fig. 4). Although the uptake of ACNPs and CNPs was higher than that of NPs, most of ACNPs and CNPs were colocalized with endosomes, suggesting the uptake of both ACNPs and CNPs was mediated by endosomes. However, different from ACNPs and CNPs, most of AnNPs were distributed in cytoplasm rather than in endosomes. Receptor mediated uptake was mainly dependent on clathrin-mediated endocytosis pathway, which was one of the endosome-mediated internalization (Mahmoudi et al., 2011). However, receptor mediated uptake often showed quick escape from the endosomes, that is why AnNPs showed poor colocalization with endosomes (Gao et al., 2013a). Combining the effect of angiopep-2 and ACP, some of the AnACNPs were colocalized with endosomes, but most of the AnACNPs were distributed in cytoplasm. The result demonstrated the dual modification could not only increase the cellular uptake but also elevate the escape efficiency from endosomes, which was consistent with previous reports (Gao et al., 2013a; Gao et al., 2014a). This property was useful for the systems delivering drugs or genes into cytoplasm and nuclei, because the endosome escape is a serious concern in gene delivery (Lu et al., 2006).

3.5. In vivo imaging

In vivo imaging was performed to determine the U-87MG xenografts targeting efficiency of different kinds of nanoparticles.

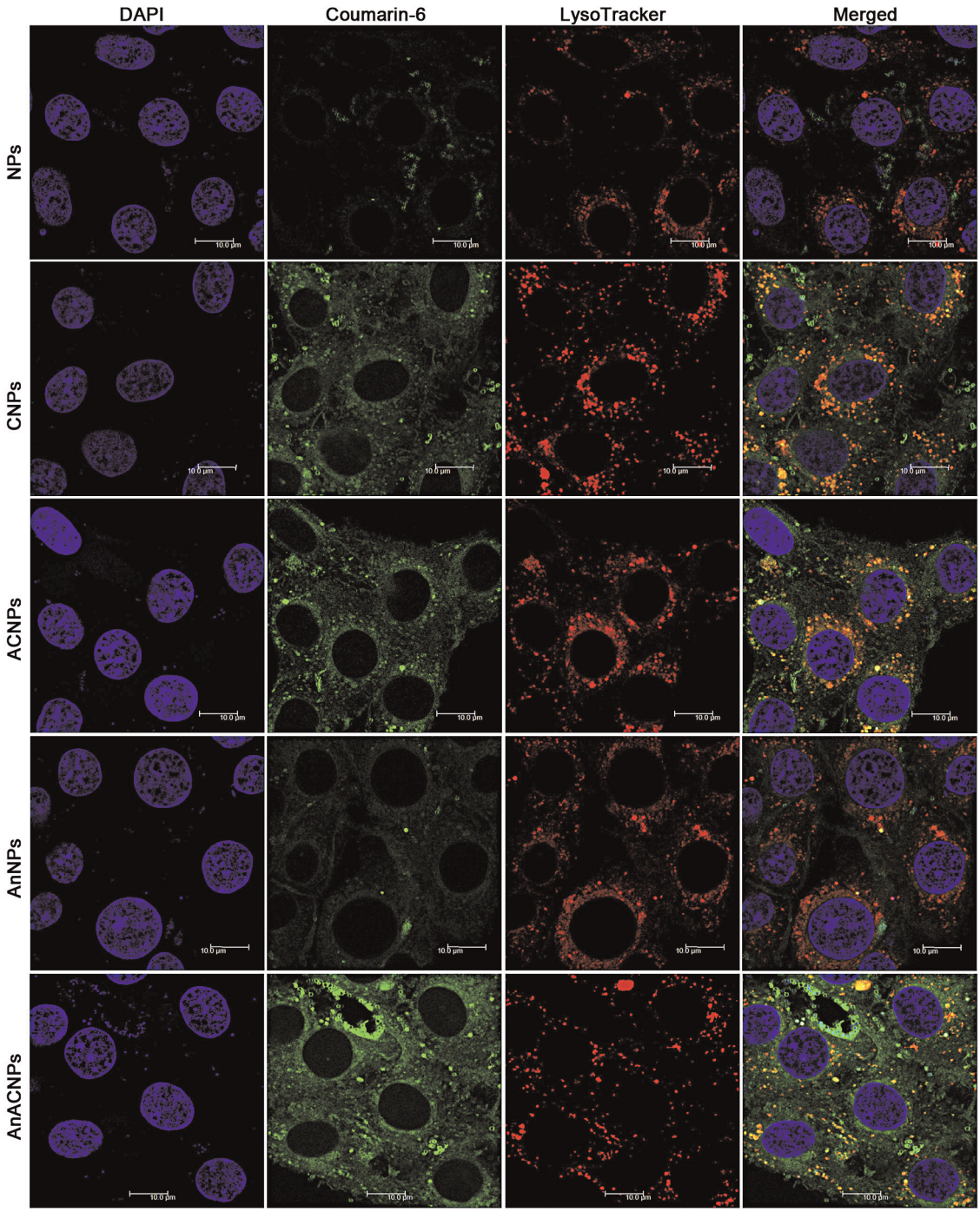

Fig. 4. Subcellular colocalization of endosomes with NPs, ACNPs, CNPs, AnNPs and AnACNPs.

2 h after administration, NPs could obviously distribute into tumor through EPR effect (Fig. 5A). However, the intensity of NPs in tumor was considerably lower than that of ACNPs and CNPs, suggesting the ACP and R8 could improve the targeting ability of nanoparticles (Jiang et al., 2004). The targeting ability of ACP and R8 was attributed to their cell penetrating property. When ACNPs and CNPs passively distributed into the tumor, ACP and R8 could facilitate the uptake by tumor cells, thus, decreasing the concentration in the interspace among tumor cells and resulting in more particles passively distributed into tumor from tumor vessels. However, due to the poor selectivity, R8 may increase the distribution in normal tissues (Fig. 5B). For example, the distribution of CNPs in liver was much higher than that of NPs, which was consistent with previous study (Gao et al., 2014b; Qin et al., 2011). In contrast, the cell penetrating property could be activated in MMP-2 overexpressed tumor, thus the distribution of ACNPs in liver was lower than that of CNPs. The lower distribution of ACNPs in normal tissues may decrease the side effects caused by CNPs.

Angiopep-2 could target tumor through the mediation of LRP1. Functionalization nanoparticles with specific ligand could improve the recognition and internalization by receptors on tumor cells, leading to elevated tumor localization (Gao et al., 2014c). Thus the distribution of AnNPs in tumor was higher than that of NPs

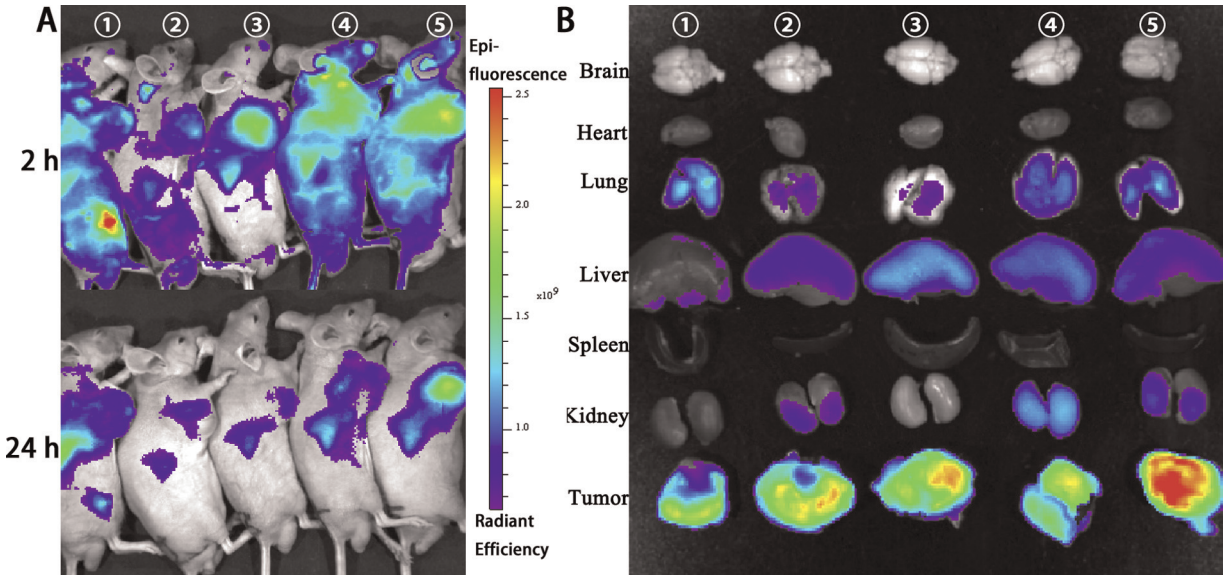

Fig. 5. A: In vivo imaging of U-87MG xenografts bearing mice. B: Ex vivo imaging of various tissues from mice, which were administrated with different kinds of nanoparticles. 1: NPs, 2: ACNPs, 3: CNPs, 4: AnNPs, 5: AnACNPs.

(Fig. 5A), which was also demonstrated by the ex vivo imaging (Fig. 5B). Combining the effect of ACP and angiopep-2, AnACNPs displayed the highest tumor localization, which was also demonstrated by ex vivo imaging. These results suggested, dual modification with different functional ligands was superior to single modification. That might be the reason that more and more researchers dedicated their effort on multi-functional drug delivery systems (Gao et al., 2014d; Kluza et al., 2012; Yan et al., 2012).

The distribution in normal tissues was further evaluated by fluorescent microscope (Fig. 6). The distributions of all particles in liver and spleen were higher than the distributions in other tissues

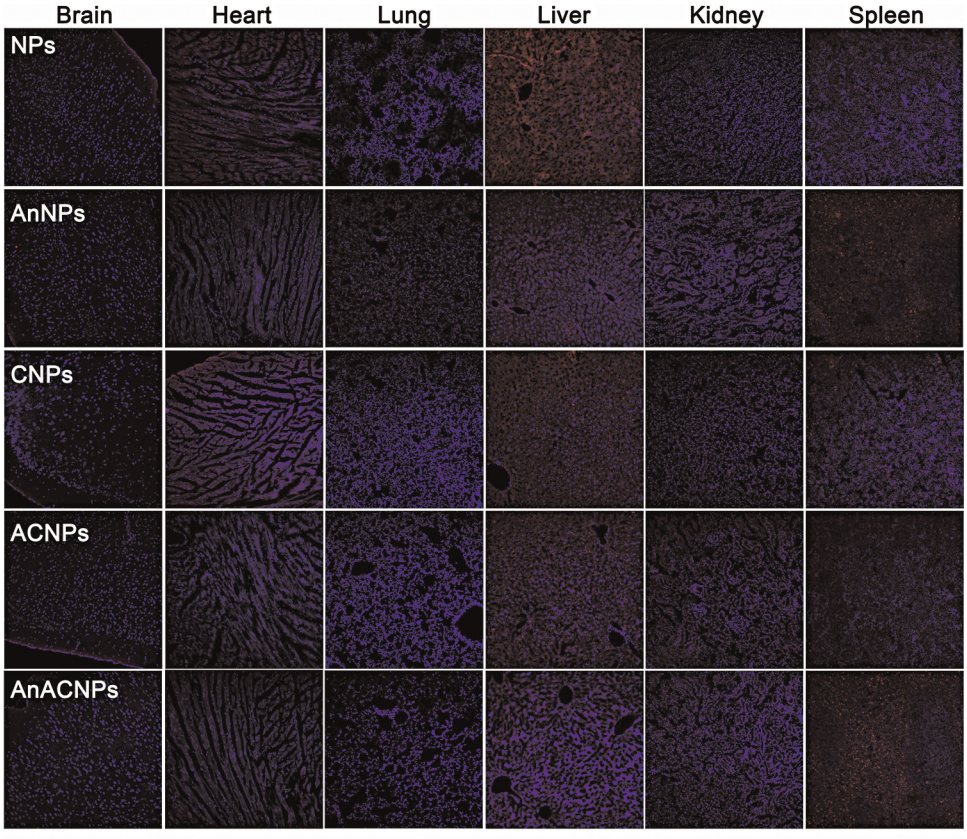

Fig. 6. Fluorescent distribution of different particles in slices of various tissues. Bar represents 100 μm.

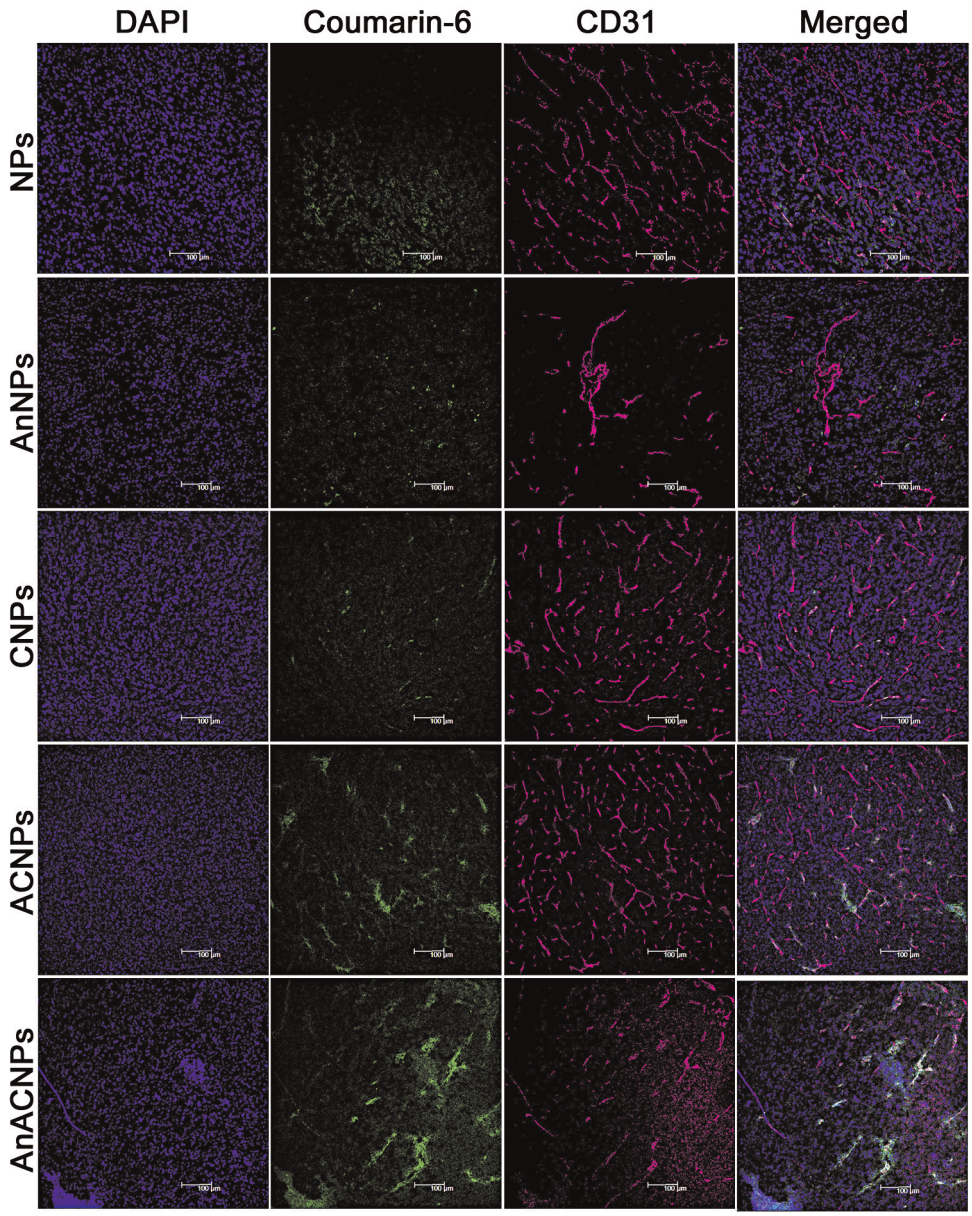

Fig. 7. Distribution of particles in tumor. Blue represents nuclei stained by DAPI, green represents coumarin-6-laoded particles and pink represents microvessel stained by anti-CD31 antibody. Bar represents 100 μm.(For interpretation of the references to colour in this figure legend, the reader is referred to the web version of this article.)

because these two are the main organs to eliminate foreign materials. The distribution of CNPs in heart was higher than that of ACNPs, suggesting ACNPs may have possessed lower heart toxicity than CNPs.

3.6. Tumor distribution

Microvessels in tumor were stained using anti-CD31 antibody (Gao et al., 2014c). The distribution of NPs in tumor was low than that of other particles (Fig. 7), which was consistent with in vivo and ex vivo imaging results. Both NPs and AnNPs showed poor colocalization with micovessels, suggesting most of NPs and AnNPs distributed in tumor cells. In contrast, both CNPs and ACNPs showed well colocalization with microvessel because the cell penetrating property of ACP and R8 led to the quick internalization of the ACNPs and CNP by cells near the microvessel when the ACNPs and CNPs passively diffused from the vessel into the tumor. Therefore, AnACNPs showed high colocalization with microvessel, and there was also significant distribution of AnACNPs in tumor cells. These results further demonstrated the dual modification could enhance the tumor targeting efficiency and increase the internalization by tumor cells.

4. Conclusion

In this study, a novel dual drug delivery system was constructed through dual modification of nanoparticles with angiopep-2 and ACP. In vitro study demonstrated the ACP could be activated at the presence of MMP-2. Dual modification system showed the highest cellular uptake and tumor targeting efficiency. Therefore, AnACNPs could serve as an efficient tumor drug delivery system.

Acknowledgements

The work was granted by National Natural Science Foundation of China (81373337), National Basic Research Program of China (973 Program, 2013CB932504) and the Sichuan University Starting Foundation for Young Teachers (2014SCU11044).

References

Alberici, L., Roth, L., Sugahara, K.N., Agemy, L., Kotamraju, V.R., Teesalu, T., Bordignon, C., Traversari, C., Rizzardi, G.P., Ruoslahti, E., 2013. De novo design of a tumor-penetrating peptide. Cancer Res. 73, 804–812.

Bae, Y.H., Park, K., 2011. Targeted drug delivery to tumors: myths, reality and possibility. J. Control. Release 153, 198–205.

Barenholz, Y.C., 2012. Doxil® – the first FDA-approved nano-drug: lessons learned. J. Control. Release 160, 117–134.

Debbage, P., 2009. Targeted drugs and nanomedicine: present and future. Curr. Pharm. Des. 15, 153–172.

Demeule, M., Currie, J.C., Bertrand, Y., Che, C., Nguyen, T., Regina, A., Gabathuler, R., Castaigne, J.P., Beliveau, R., 2008. Involvement of the low-density lipoprotein receptor-related protein in the transcytosis of the brain delivery vector angiopep-2. J. Neurochem. 106, 1534–1544.

Fang, J., Nakamura, H., Maeda, H., 2011. The EPR effect: unique features of tumor blood vessels for drug delivery, factors involved, and limitations and augmentation of the effect. Adv. Drug Deliv. Rev. 63, 136–151.

Florence, A.T., 2012. Targeting nanoparticles: the constraints of physical laws and physical barriers. J. Control. Release 164, 115–124.

Foged, C., Nielsen, H.M., 2008. Cell-penetrating peptides for drug delivery across membrane barriers. Exp. Opin. Drug Deliv. 5, 105–117.

Forsyth, P.A., Wong, H., Laing, T.D., Rewcastle, N.B., Morris, D.G., Muzik, H., Leco, K.J., Johnston, R.N., Brasher, P.M., Sutherland, G., Edwards, D.R., 1999. Gelatinase-A (MMP-2), gelatinase-B (MMP-9) and membrane type matrix metalloproteinase-1 (MT1-MMP) are involved in different aspects of the pathophysiology of malignant gliomas. Br. J. Cancer 79, 1828–1835.

Gao, H., Pan, S., Yang, Z., Cao, S., Chen, C., Jiang, X., Shen, S., Pang, Z., Hu, Y., 2011. A cascade targeting strategy for brain neuroglial cells employing nanoparticles modified with angiopep-2 peptide and EGFP-EGF1 protein. Biomaterials 32, 8669–8675.

Gao, H., Yang, Z., Zhang, S., Cao, S., Shen, S., Pang, Z., Jiang, X., 2013a. Ligand modified nanoparticles increases cell uptake, alters endocytosis and elevates glioma distribution and internalization. Sci. Rep. 3, 2534.

Gao, H., Cao, S., Chen, C., Cao, S., Yang, Z., Pang, Z., Xi, Z., Pan, S., Zhang, Q., Jiang, X., 2013b. Incorporation of lapatinib into lipoprotein-like nanoparticles with enhanced water solubility and anti-tumor effect in breast cancer. Nanomedicine (Lond.) 8, 1429–1442.

Gao, W., Xiang, B., Meng, T.T., Liu, F., Qi, X.R., 2013c. Chemotherapeutic drug delivery to cancer cells using a combination of folate targeting and tumor microenvironment-sensitive polypeptides. Biomaterials 34, 4137–4149.

Gao, H., Zhang, S., Cao, S., Yang, Z., Pang, Z., Jiang, X., 2014a. Angiopep-2 and activatable cell-penetrating peptide dual-functionalized nanoparticles for systemic glioma-targeting delivery. Mol. Pharm.

Gao, H., Yang, Z., Zhang, S., Pang, Z., Liu, Q., Jiang, X., 2014b. Study and evaluation of mechanisms of dual targeting drug delivery system with tumor microenvironment assays compared with normal assays. Acta Biomater. 10, 858–867.

Gao, H., Xiong, Y., Zhang, S., Yang, Z., Cao, S., Jiang, X., 2014c. RGD and interleukin-13 peptide functionalized nanoparticles for enhanced glioblastoma cells and neovasculature dual targeting delivery and elevated tumor penetration. Mol. Pharm. 11, 1042–1052.

Gao, H., Yang, Z., Cao, S., Xiong, Y., Zhang, S., Pang, Z., Jiang, X., 2014d. Tumor cells and neovasculature dual targeting delivery for glioblastoma treatment. Biomaterials 35, 2374–2382.

Hobbs, S.K., Monsky, W.L., Yuan, F., Roberts, W.G., Griffith, L., Torchilin, V.P., Jain, R.K., 1998. Regulation of transport pathways in tumor vessels: role of tumor type and microenvironment. Proc. Natl. Acad. Sci. U. S. A. 95, 4607–4612.

Ito, S., Ohtsuki, S., Terasaki, T., 2006. Functional characterization of the brain-to-blood efflux clearance of human amyloid-beta peptide (1–40) across the rat blood–brain barrier. Neurosci. Res. 56, 246–252.

Jiang, T., Olson, E.S., Nguyen, Q.T., Roy, M., Jennings, P.A., Tsien, R.Y., 2004. Tumor imaging by means of proteolytic activation of cell-penetrating peptides. Proc. Natl. Acad. Sci. U. S. A. 101, 17867–17872.

Kluza, E., Jacobs, I., Hectors, S.J., Mayo, K.H., Griffioen, A.W., Strijkers, G.J., Nicolay, K., 2012. Dual-targeting of alphavbeta3 and galectin-1 improves the specificity of paramagnetic/fluorescent liposomes to tumor endothelium in vivo. J. Control. Release 158, 207–214.

Kondo, E., Saito, K., Tashiro, Y., Kamide, K., Uno, S., Furuya, T., Mashita, M., Nakajima, K., Tsumuraya, T., Kobayashi, N., Nishibori, M., Tanimoto, M., Matsushita, M., 2012. Tumour lineage-homing cell-penetrating peptides as anticancer molecular delivery systems. Nat. Commun. 3, 951.

Kuai, R., Yuan, W., Li, W., Qin, Y., Tang, J., Yuan, M., Fu, L., Ran, R., Zhang, Z., He, Q., 2011. Targeted delivery of cargoes into a murine solid tumor by a cell-penetrating peptide and cleavable poly(ethylene glycol) comodified liposomal delivery system via systemic administration. Mol. Pharm. 8, 2151–2161.

Lammers, T., Kiessling, F., Hennink, W.E., Storm, G., 2012. Drug targeting to tumors: principles, pitfalls and (pre-) clinical progress. J. Control. Release 161, 175–187.

Liu, Y., Ji, M., Wong, M.K., Joo, K.I., Wang, P., 2013. Enhanced therapeutic efficacy ofiRGD-conjugated crosslinked multilayer liposomes for drug delivery. Biomed. Res. Int. 2013, 1–11.

Liu, Y., Kim, Y.J., Ji, M., Fang, J., Siriwon, N., Zhang, L.I., Wang, P., 2014a. Enhancing gene delivery of adeno-associated viruses by cell-permeable peptides. Mol. Ther. Methods Clin. Dev. 1, 12.

Liu, Y., Ran, R., Chen, J., Kuang, Q., Tang, J., Mei, L., Zhang, Q., Gao, H., Zhang, Z., He, Q., 2014b. Paclitaxel loaded liposomes decorated with a multifunctional tandem peptide for glioma targeting. Biomaterials 35, 4835–4847.

Lu, W., Zhang, Y., Tan, Y.Z., Hu, K.L., Jiang, X.G., Fu, S.K., 2005. Cationic albumin-conjugated pegylated nanoparticles as novel drug carrier for brain delivery. J. Control. Release 107, 428–448.

Lu, W., Sun, Q., Wan, J., She, Z., Jiang, X.G., 2006. Cationic albumin-conjugated pegylated nanoparticles allow gene delivery into brain tumors via intravenous administration. Cancer Res. 66, 11878–11887.

Mahmoudi, M., Azadmanesh, K., Shokrgozar, M.A., Journeay, W.S., Laurent, S., 2011. Effect of nanoparticles on the cell life cycle. Chem. Rev. 111, 3407–3432.

Maletinska, L., Blakely, E.A., Bjornstad, K.A., Deen, D.F., Knoff, L.J., Forte, T.M., 2000. Human glioblastoma cell lines: levels of low-density lipoprotein receptor and low-density lipoprotein receptor-related protein. Cancer Res. 60, 2300–2303.

Marcucci, F., Lefoulon, F., 2004. Active targeting with particulate drug carriers in tumor therapy: fundamentals and recent progress. Drug Discov. Today 9, 219–228.

Matsumura, Y., Maeda, H., 1986. A new concept for macromolecular therapeutics in cancer chemotherapy: mechanism of tumoritropic accumulation of proteins and the antitumor agent smancs. Cancer Res. 46, 6387–6392.

Olson, E.S., Jiang, T., Aguilera, T.A., Nguyen, Q.T., Ellies, L.G., Scadeng, M., Tsien, R.Y., 2010. Activatable cell penetrating peptides linked to nanoparticles as dual probes for in vivo fluorescence and MR imaging of proteases. Proc. Natl. Acad. Sci. U. S. A. 107, 4311–4316.

Pang, Z., Lu, W., Gao, H., Hu, K., Chen, J., Zhang, C., Gao, X., Jiang, X., Zhu, C., 2008. Preparation and brain delivery property of biodegradable polymersomes conjugated with OX26. J. Control. Release 128, 120–127.

Qin, Y., Chen, H., Yuan, W., Kuai, R., Zhang, Q., Xie, F., Zhang, L., Zhang, Z., Liu, J., He, Q., 2011. Liposome formulated with TAT-modified cholesterol for enhancing the brain delivery. Int. J. Pharm. 419, 85–95.

Svensen, N., Walton, J.G., Bradley, M., 2012. Peptides for cell-selective drug delivery. Trends Pharmacol. Sci. 33, 186–192.

Tang, J., Zhang, L., Liu, Y., Zhang, Q., Qin, Y., Yin, Y., Yuan, W., Yang, Y., Xie, Y., Zhang, Z., He, Q., 2013. Synergistic targeted delivery of payload into tumor cells by dual-ligand liposomes co-modified with cholesterol anchored transferrin and TAT. Int. J. Pharm. 454, 31–40.

Xin, H., Jiang, X., Gu, J., Sha, X., Chen, L., Law, K., Chen, Y., Wang, X., Jiang, Y., Fang, X., 2011. Angiopep-conjugated poly(ethylene glycol)-co-poly(epsilon-caprolactone) nanoparticles as dual-targeting drug delivery system for brain glioma. Biomaterials 32, 4293–4305.

Yan, H., Wang, L., Wang, J., Weng, X., Lei, H., Wang, X., Jiang, L., Zhu, J., Lu, W., Wei, X., Li, C., 2012. Two-order targeted brain tumor imaging by using an optical/paramagnetic nanoprobe across the blood brain barrier. ACS Nano 6, 410–420.

van der Meel, R., Vehmeijer, L.J., Kok, R.J., Storm, G., van Gaal, E.V., 2013. Ligand-targeted particulate nanomedicines undergoing clinical evaluation: current status. Adv. Drug Deliv. Rev. 65, 1284–1298.